



## MATHEMATICAL ANALYSIS OF TYPHOID-HCV CO-INFECTION TRANSMISSION DYNAMICS

Olawuyi O. M.<sup>1</sup>, Isobeye G.<sup>2</sup>, and Abegye S. Y.<sup>3\*</sup>

<sup>1</sup>Department of Mathematics, Alvan Ikoku Federal University of Education, Owerri, Imo, Nigeria.

<sup>2</sup>Department of Mathematics, Ajuru University of Education, Rumuolumeni, Port Harcourt, Rivers, Nigeria.

<sup>3</sup>Department of Mathematics and Statistics, Isa Mustapha Agwai 1 Polytechnic, Lafia, Nigeria.

\*Corresponding Author's Email: [yakubupurity@gmail.com](mailto:yakubupurity@gmail.com)

### Cite this article:

Olawuyi, O. M., Isobeye, G., Abegye, S. Y. (2026), Mathematical Analysis of Typhoid-HCV Co-Infection Transmission Dynamics. African Journal of Mathematics and Statistics Studies 9(2), 11-40. DOI: 10.52589/AJMSS-53NHWL43

### Manuscript History

Received: 13 Mar 2026

Accepted: 14 Apr 2026

Published: 19 May 2026

### Copyright © 2026 The Author(s).

This is an Open Access article distributed under the terms of Creative Commons Attribution-NonCommercial-NoDerivatives 4.0 International (CC BY-NC-ND 4.0), which permits anyone to share, use, reproduce and redistribute in any medium, provided the original author and source are credited.

**ABSTRACT:** *The World Health Organization had strategized a global eradication of hepatitis C virus (HCV) since 2016 because of its impact on global population. Its elimination has been prolonged because it was discovered that the diseases can co-exist with Typhoid fever and both illnesses contributing significantly to morbidity and long-term health complications. Therefore, a study was conducted using a compartmental model to explain the transmission dynamics of this co-infection leading to a non – linear deterministic equation. The basic reproduction number ( $\mathcal{R}_0$ ) was obtained by next-generation method and the two criteria for stability conditions were computed. The free equilibrium point was evaluated and showed to be locally asymptotically stable when the threshold quantity is less than one. It was shown that both the analytical and numerical results agree with each other's. Also, the results revealed that the susceptible population initially dominated but gradually declined as infection spread, while the recovered class steadily increased due to effective treatment and vaccination. Co-infection levels ( $A_C$ ) remained low but persistent without control, confirming the synergistic effect of both pathogens.*

**KEYWORDS:** Co-infection, stability, basic reproduction number, sensitivity analysis.



## INTRODUCTION

Hepatitis C Virus (HCV) is a viral liver disease transmitted primarily through exposure to infected blood, such as sharing needles, unsafe blood transfusions, and the use of unsterilized medical instruments (Elamin, 2013). Key factors influencing its spread include poor medical safety practices, blood exposure, and limited screening programs. HCV is treatable with antiviral drugs, which can cure many infections and prevent severe liver complications (Mlyashimb et al., 2025).

Typhoid fever, on the other hand, is a bacterial infection caused by *Salmonella typhi*, transmitted through contaminated food and water, often due to poor sanitation and hygiene (Abah, 2023). Its spread is largely influenced by unsafe drinking water, poor waste disposal systems, and inadequate hygiene practices. Treatment typically involves antibiotics, proper hydration, and rest, while preventive measures include access to clean water, improved sanitation, and vaccination (Enejoh et al., 2026).

The co-infection of HCV and typhoid fever represents a significant public health challenge, particularly in developing countries where both diseases are endemic. These infections affect different but critical body systems—the liver and gastrointestinal tract—and may present overlapping symptoms, thereby complicating diagnosis and treatment. Socio-economic factors such as poverty, inadequate sanitation, and limited access to healthcare services further increase the likelihood of co-infection within affected populations.

Globally, the burden of these diseases remains high. The World Health Organization (WHO, 2024) estimates that approximately 58 million people are living with chronic HCV infection, with about 1.5 million new infections occurring annually. Similarly, typhoid fever continues to pose a major health risk, with an estimated 11–21 million cases and 128,000–161,000 deaths reported each year worldwide (WHO, 2025). In Africa, hundreds of thousands of new typhoid cases are recorded annually, particularly in regions with poor water supply and sanitation infrastructure, including Nigeria.

In countries like Nigeria, where blood-borne infections such as HCV coexist with water-borne diseases like typhoid fever, the possibility of simultaneous infection is high. Limited screening programs, inadequate healthcare access, and poor environmental conditions contribute significantly to the persistence and overlap of these diseases. Evidence of such co-infections has been reported in Uyo, Akwa Ibom State, Nigeria, where cases were documented in recent medical literature (Olajide et al., 2025).

Although several studies have examined co-infections involving typhoid fever or HCV with other diseases, there is limited research specifically addressing the co-dynamics of HCV and typhoid fever within a unified modeling framework. For instance, Zeleke et al. (2021) developed an ODE model for the co-infection of *Plasmodium falciparum* and *Salmonella typhi*, analyzing equilibrium states and the basic reproduction number. Lunga and Farai (2022) investigated typhoid–cholera co-infection dynamics and demonstrated that simultaneous control strategies are most effective. Mamo et al. (2022) modeled Hepatitis A and typhoid co-infection using optimal control techniques, while Daniel et al. (2025) studied COVID-19 and typhoid co-dynamics, emphasizing the role of treatment and screening in reducing transmission. In a related study, Oluwakemi et al. (2022) examined HIV–HCV co-



infection and showed that improved treatment significantly reduces disease spread and complications.

Despite these contributions, there remains a significant gap in the literature regarding the mathematical modeling of HCV and typhoid fever co-infection. This study aims to address this gap by developing and analyzing a unified model for the co-infection dynamics of HCV and typhoid fever, with particular focus on Uyo, Akwa Ibom State, Nigeria.

### Model development

The population is classified into eight compartments: the susceptible represented by  $S(t)$ , exposed Typhoid  $E_T(t)$ , acute typhoid  $A_T(t)$ , exposed HCV  $E_H(t)$ , acute HCV  $A_H(t)$ , acute typhoid-HCV co-infection  $A_C(t)$ , those who had recovered from infected population  $R(t)$  and bacteria population  $B(t)$  all in time  $t$ . The entire human population size  $N(t)$  can be described as:

$$N(t) = S(t) + E_T(t) + A_T(t) + E_H(t) + A_H(t) + A_C(t) + R(t)$$

We assumed that individuals enter the susceptible class through recruitment at rate  $\Lambda$ . Susceptible individuals acquire Typhoid through contact with contaminated bacteria or infected individuals with force of infection  $\lambda_T$ , and HCV through contact with infected individuals with force of infection  $\lambda_H$  expressed as

$$\lambda_T = \beta_T \left( \frac{\eta_1 A_T + \eta_2 A_C + B}{N} \right) \quad (1)$$

$$\lambda_H = \beta_H \left( \frac{A_H + A_C}{N} \right) \quad (2)$$

Typhoid infection progresses from exposed  $E_T$  to acute Typhoid  $A_T$ , while HCV infection progresses from exposed  $E_H$  to acute HCV  $A_H$ . Individuals in the acute classes may recover, die naturally, or die due to disease. Co-infection occurs when individuals in the acute Typhoid class acquire HCV or when acute HCV individuals acquire Typhoid, moving them into the co-infected class  $A_C$ . Co-infected individuals may recover, partially regress to single infection classes, or die. Typhoid bacteria are shed into the environment by infected individuals and decay naturally, contributing to further transmission.

The proposed model is described in Fig. 1. Using the diagram and the model's description, the governing mathematical dynamics can be shown as system of odes as:

$$\frac{dS}{dt} = \Lambda - (\lambda_T + \lambda_H + \mu)S$$

$$\frac{dE_T}{dt} = \lambda_T S - (\sigma_1 + \mu)E_T$$

$$\frac{dA_T}{dt} = \sigma_1 E_T + \theta_1 A_C - \lambda_H A_T - (\gamma_1 + \delta_1 + \mu)A_T$$

$$\frac{dE_H}{dt} = \lambda_H S - (\sigma_2 + \mu)E_H$$

$$\frac{dA_H}{dt} = \sigma_2 E_H + \theta_2 A_C - \lambda_T A_H - (\gamma_2 + \delta_2 + \mu) A_H \tag{3}$$

$$\frac{dA_C}{dt} = \lambda_H A_T + \lambda_T A_H - (\gamma_3 + \theta_1 + \theta_2 + \delta_3 + \mu) A_C$$

$$\frac{dR}{dt} = \gamma_1 A_T + \gamma_2 A_H + \gamma_3 A_C - \mu R$$

$$\frac{dB}{dt} = \epsilon_1 A_T + \epsilon_2 A_C - \tau B$$

where  $\lambda_T$  and  $\lambda_H$  are given in (1) and (2) with initial conditions  $S(0) = S_0 > 0, E_T(0) = E_{T0} \geq 0, A_T(0) = A_{T0} \geq 0, E_H(0) = E_{H0} \geq 0, A_H(0) = A_{H0} \geq 0, A_C(0) = A_{C0} \geq 0, B(0) = B_0 \geq 0, R(0) = R_0 \geq 0$ . The parameters descriptions of the model with their values and sources are shown in Table 1.

**Figure 1: The schematic diagram of HCV-Typhoid co-infection model**

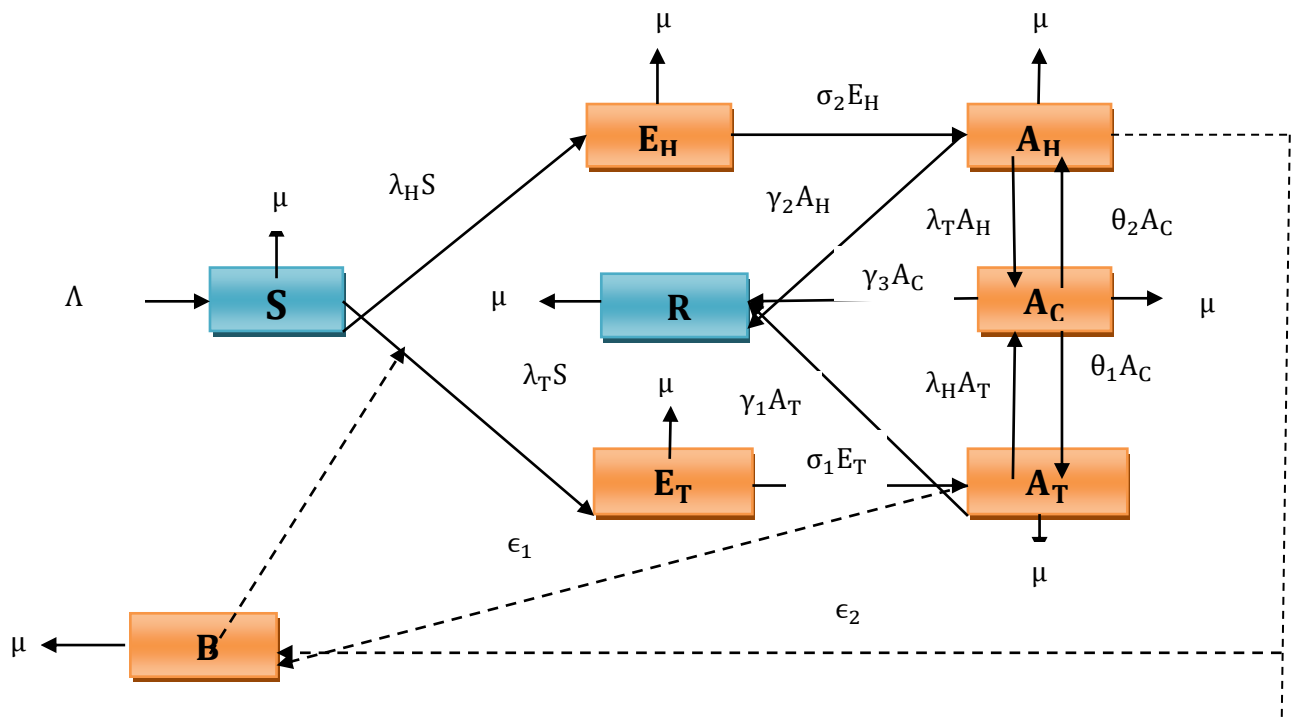


**Table 1: The values of parameters and sources**

Parameters	Values	Sources
$\Lambda$	49.9	Daniel et al, (2025)
$\mu$	0.00005	Olajide et al, (2025)
$\beta_T$	0.5	Olajide et al, (2025)
$\beta_H$	0.6	Olajide et al, (2025)
$\sigma_1$	0.1	Thierry et al, (2025)
$\sigma_2$	0.08	Olajide et al, (2025)
$\gamma_1$	0.05	Thierry et al, (2025)
$\gamma_2$	0.04	Enejoh et al, (2026)



$\gamma_3$	0.03	Olajide et al, (2025)
$\delta_1$	0.01	Thierry et al, (2025)
$\delta_2$	0.02	Enejoh et al, (2026)
$\delta_3$	0.02	Olajide et al, (2025)
$\theta_1$	0.01	Estimated
$\theta_2$	0.02	Estimated
$\epsilon_1$	0.05	Olajide et al, (2025)
$\epsilon_2$	0.03	Olajide et al, (2025)
$\tau$	0.5	Mlyashimb & Adquate, (2025)
$K$	100	Thierry et al, (2025)
$\eta_1$	0.4	Daniel et al, (2025)
$\eta_2$	0.5	Daniel et al, (2025)

### The Properties of the Model

This section presents the basic preliminary properties of the system that plays a significant role in ascertaining the existence and uniqueness of the solution.

#### Uniqueness of solution of the model

We adopt the approach used by Keno et al, (2023) in order to construct the uniqueness of the model solution applied as follows:

The general first order ODE is usually represented as:

$$x' = z(x, t), x(0) = x_0 \quad (4)$$

In considering the existence and uniqueness solution, an individual will be inquisitive to know the following:

- the precise condition for the existence of the solution of the modeled equation
- the precise condition for the uniqueness of the solution of the modeled equation

These basic facts above can be addressed by the following, let

$$\begin{aligned}
 z_1 &= \Lambda - (\lambda_T + \lambda_H + \mu)S \\
 z_2 &= \lambda_T S - (\sigma_1 + \mu)E_T \\
 z_3 &= \sigma_1 E_T + \theta_1 A_c - \lambda_H A_T - (\gamma_1 + \delta_1 + \mu)A_T \\
 z_4 &= \lambda_H S - (\sigma_2 + \mu)E_H \\
 z_5 &= \sigma_2 E_H + \theta_2 A_c - \lambda_T A_H - (\gamma_2 + \delta_2 + \mu)A_H \\
 z_6 &= \lambda_H A_T + \lambda_T A_H - (\gamma_3 + \theta_1 + \theta_2 + \delta_3 + \mu)A_c
 \end{aligned} \quad (5)$$



$$z_7 = \gamma_1 A_T + \gamma_2 A_H + \gamma_3 A_C - \mu R$$

$$z_8 = \epsilon_1 A_T + \epsilon_2 A_C - \tau B$$

The uniqueness and existence properties of the model can be shown using the theorems below:

**Theorem 2.1.1** Consider  $D$  to be a domain as treated in Inayaturohmat et al, (2022).

$$|t - t_0| \leq C \|y - y_0\| < d \quad (6)$$

Where  $y = (y_1, y_2, \dots, y_n)$ ,  $y_0 = (y_{10}, y_{20}, \dots, y_{n0})$  and  $z(x, t)$  satisfies Lipschitz condition.

$$\|z(t, y_1) - z(t, y_2)\| \leq M \|y_1 - y_2\| \quad (7)$$

It follows that the ordered pairs  $(t, y_1)$  and  $(t, y_2)$  are in the domain  $D$ , where  $M \geq 0$ , therefore, there exist a positive constant  $\delta$  and a unique continuous vector solution  $y(t)$  of the modeled system in the interval  $|t - t_0| \leq \delta$ . It worth nothing the condition of our modeled system, is satisfied by  $\left\{ \frac{dz_i}{dy_j} =: i, j = 1, 2, \dots, n \right\}$  is continuous and bounded in the domain  $D$ . If  $z(t, y)$  is a continuous partial derivative  $\frac{dz_i}{dy_j}$  on a bounded closed convex domain  $V$ , where  $V$  is the real number, then it satisfied Lipschitz criteria in  $V$ . We desire that the domain in  $\mathfrak{R} \in [1, V]$ . Hence, we seek for a bounded solution  $V > 0$ . So, we prove the existence theorem below.

### Existence of the solution of the model

**Theorem 2.1.2** Let  $D$  be the domain defined in the system 3 holds. Hence, there exists a solution of the modeled system which is bounded in the domain  $D$ .

**Proof:** Using systems 5 above, we show that  $\left\{ \frac{dz_i}{dy_j} =: i, j = 1, 2, \dots, 12 \right\}$  are continuous and consequently bounded which were obtained by taking their partial derivative of the system 5.

$$\frac{\partial z_1}{\partial S} = |-(\lambda_T + \lambda_H + \mu)| < \infty, \frac{\partial z_1}{\partial E_T} = \frac{\partial z_1}{\partial E_H} = \frac{\partial z_1}{\partial A_H} = \frac{\partial z_1}{\partial R} = |0| < \infty, \frac{\partial z_1}{\partial A_C} = \left| -\beta_T \frac{\eta_2 S}{N} \right| < \infty,$$

$$\frac{\partial z_1}{\partial B} = \left| -\frac{\beta_T S}{N} \right| < \infty$$

$$\frac{\partial z_2}{\partial S} = |\lambda_T| < \infty, \frac{\partial z_2}{\partial E_T} = |-(\delta_1 + \mu)| < \infty, \frac{\partial z_2}{\partial E_H} = \frac{\partial z_2}{\partial A_H} = \frac{\partial z_2}{\partial R} = |0| < \infty, \frac{\partial z_2}{\partial A_T} = \left| \beta_T \frac{\eta_1 S}{N} \right| < \infty, \frac{\partial z_2}{\partial A_C} = \left| \beta_T \frac{\eta_2 S}{N} \right| < \infty, \frac{\partial z_2}{\partial B} = \left| \frac{\beta_T S}{N} \right| < \infty$$

$$\frac{\partial z_3}{\partial S} = \frac{\partial z_3}{\partial E_H} = \frac{\partial z_3}{\partial A_H} = \frac{\partial z_3}{\partial R} = \frac{\partial z_3}{\partial B} = |0| < \infty, \frac{\partial z_3}{\partial E_T} = |\sigma_1| < \infty, \frac{\partial z_3}{\partial A_T} = |-(\lambda_H + \gamma_1 + \delta_1 + \mu)| < \infty,$$

$$\frac{\partial z_3}{\partial A_C} = |\theta_1| < \infty$$



$$\frac{\partial z_4}{\partial S} = |\lambda_H| < \infty, \frac{\partial z_4}{\partial E_T} = \frac{\partial z_4}{\partial A_T} = \frac{\partial z_4}{\partial R} = \frac{\partial z_4}{\partial B} = |0| < \infty, \frac{\partial z_4}{\partial E_H} = |-(\sigma_2 + \mu)| < \infty, \frac{\partial z_4}{\partial A_H} = \frac{\partial z_4}{\partial A_C} = \left| \frac{\beta_H S}{N} \right| < \infty,$$

$$\frac{\partial z_5}{\partial S} = \frac{\partial z_5}{\partial E_T} = \frac{\partial z_5}{\partial A_T} = \frac{\partial z_5}{\partial R} = \frac{\partial z_5}{\partial B} = |0| < \infty, \frac{\partial z_5}{\partial E_H} = |\sigma_2| < \infty, \frac{\partial z_5}{\partial A_H} = |-(\lambda_H + \gamma_2 + \delta_2 + \mu)| < \infty, \frac{\partial z_5}{\partial A_C} = |\theta_2| < \infty$$

$$\frac{\partial z_6}{\partial A_T} = |\lambda_H| < \infty, \frac{\partial z_6}{\partial A_H} = |-(\tau_2 + \theta_2 + \delta_3 + \mu)| < \infty, \frac{\partial z_6}{\partial S} = \frac{\partial z_6}{\partial E_T} = \frac{\partial z_6}{\partial E_H} = \frac{\partial z_6}{\partial R} = \frac{\partial z_6}{\partial B} = |0| < \infty, \frac{\partial z_6}{\partial A_H} = |\lambda_T| < \infty,$$

$$\frac{\partial z_7}{\partial A_T} = |\gamma_1| < \infty, \frac{\partial z_7}{\partial A_H} = |\gamma_2| < \infty, \frac{\partial z_7}{\partial A_C} = |\gamma_3| < \infty, \frac{\partial z_7}{\partial R} = |-\mu| < \infty, \frac{\partial z_7}{\partial S} = \frac{\partial z_7}{\partial E_T} = \frac{\partial z_7}{\partial E_H} = |0| < \infty$$

$$\frac{\partial z_8}{\partial A_T} = |\epsilon_1| < \infty, \frac{\partial z_8}{\partial A_C} = |\epsilon_2| < \infty, \frac{\partial z_8}{\partial B} = |\tau| < \infty, \frac{\partial z_8}{\partial S} = \frac{\partial z_8}{\partial E_T} = \frac{\partial z_8}{\partial E_H} = \frac{\partial z_8}{\partial A_H} = \frac{\partial z_8}{\partial P} = |0| < \infty$$

It has been proved that these sixty-four (64) partial derivatives are continuous and bounded as required, which further indicated that there exist a unique solution of the system 3 within the domain D.

### Invariant region and attractiveness for the model

Since this system is concerned with human population, hence all the solution must be positive and bounded within the feasible region. In connection with this, following the theorem below:

**Theorem 2.1.3** The solutions of model 3 are positive, unique and bounded in the region

$$\Omega = (S, E_T, A_T, E_H, A_H, A_C, R, B) \in \mathbb{R}_+^8, 0 \leq N(t) \leq \frac{\Lambda}{\mu} \quad (8)$$

Proof: Using Picard-Lindelof theorem as adopted in Inayaturohmat et al, (2022), the right hand of 26 function are in  $c'$  on  $\mathbb{R}_+^8$  has a unique solution. We first need to show that the region  $\Omega$  is positively invariant, which guarantee us to consider the existence of the system of the model in  $\Omega$ . Then summing the system of 3, we have

$$\frac{dN}{dt} = \Lambda - \mu N - (\delta_1 A_T + \delta_2 A_H + \delta_3 A_C) + \epsilon_1 A_T + \epsilon_2 A_C + -\tau B \quad (9)$$

In absence of infection there will be no death ( $\delta_1, \delta_2, \delta_3 = 0$ ) and  $A_T = A_C = 0$ , hence equation (9) reduces to

$$\frac{dN}{dt} = \Lambda - \mu N$$

Hence it can be seen that  $\frac{dN}{dt} < 0$  if  $N(t) > 0$ . Therefore,



$$\frac{dN}{dt} + \mu N = \Lambda$$

Solving this equation, using integrating factor, it follows that

$$N(t) = \frac{\Lambda}{\mu} + \left(N_0 - \frac{\Lambda}{\mu}\right) e^{-\mu t} \quad (10)$$

As  $t \rightarrow \infty$ , then  $N(t) = \frac{\Lambda}{\mu}$ . Also, it implies that  $N(t) \leq N_0 e^{-\mu t} + \frac{\Lambda}{\mu} (1 - e^{-\mu t})$  from 10 which follow that  $\Omega$  is positively invariant from standard comparison theorem in Keno et al, (2023). For  $\Omega$  to be positively invariant then  $N_0 > \frac{\Lambda}{\mu}$ , then the solution enters  $\Omega$  finites times or  $N(t)$  tends to  $\frac{\Lambda}{\mu}$  asymptotically, consequently the infected populations  $E_T, A_T, E_H, A_H$  and  $A_C$  approaches to zero. Therefore,  $\Omega$  is attracting. This completes the proof.

### Positivity and bounded for the model

**Theorem 2.1.4** The solution of our system 3 is considered to be positively bounded for all  $(S(0), E_T(0), A_T(0), E_H(0), A_H(0), A_C(0), R(0), B(0)) \in \mathbb{R}_+^8$  for time  $(t) > 0$ .

**Proof:** To verify that the system is positive, then it is important to show that on every hyperplane bounding describing the vector field point is in  $\mathbb{R}_+^8$ . Using the system 3, it then follows that:

$$\left. \frac{dS}{dt} \right|_{S=0} = \Lambda \geq 0, \quad \left. \frac{dE_T}{dt} \right|_{E_T=0} = \lambda_T S \geq 0, \quad \left. \frac{dA_T}{dt} \right|_{A_T=0} = (\sigma_1 E_T + \theta_1 A_C) \geq 0, \quad \left. \frac{dE_H}{dt} \right|_{E_H=0} = \lambda_H S \geq 0,$$

$$\left. \frac{dA_H}{dt} \right|_{A_H=0} = (\sigma_2 E_H + \theta_2 A_C) \geq 0, \quad \left. \frac{dA_C}{dt} \right|_{A_C=0} = (\lambda_H A_T + \lambda_T A_H) \geq 0, \quad \left. \frac{dR}{dt} \right|_{R=0} = (\gamma_1 A_T + \gamma_2 A_H + \gamma_3 A_C) \geq 0, \quad \left. \frac{dB}{dt} \right|_{B=0} = (\epsilon_1 A_T + \epsilon_2 A_C) \geq 0$$

It follows that the solution set remains in  $\mathbb{R}_+^8$  with the bounding feasible region shown below

$$\Omega = \{(S(0), E_T(0), A_T(0), E_H(0), A_H(0), A_C(0), R(0), B(0))\} \in \mathbb{R}_+^8$$

## MODEL ANALYSIS

In order to comprehend the behavior of the coexistence of the model, we first study the sub-models of each diseases and before proceeding to compute the model equilibrium points and then examine the model dynamics around those stationary points of the co-infection.

### Typhoid Fever only model

In absence of those infected by HCV by setting  $E_H = A_H = A_C = 0$ , then Typhoid fever (TF) model reduces to

$$\frac{dS}{dt} = \Lambda - (\lambda_T + \mu)S$$



$$\begin{aligned}\frac{dE_T}{dt} &= \lambda_T S - (\sigma_1 + \mu)E_T \\ \frac{dA_T}{dt} &= \sigma_1 E_T - (\gamma_1 + \delta_1 + \mu)A_T \\ \frac{dR}{dt} &= \gamma_1 A_T - \mu R \\ \frac{dB}{dt} &= \epsilon_1 A_T - \tau B\end{aligned}\quad (11)$$

$$\text{where } \lambda_T = \beta_T \left( \frac{\eta_1 A_T}{N} + \frac{B}{K+B} \right)$$

### The local stability of Typhoid fever sub-model

System's equilibria play a very important role describing their stability which portrait whether the dynamic goes to extinction or persist. In the absence of Typhoid fever, we determinate the disease-free equilibrium point using equation 3 denoted by  $E_{0T} = \left( \frac{\Lambda}{\mu}, 0, 0, 0 \right)$ . The basic reproduction number of the sub-model connotes the average number of secondary infections produced by a single typhoid infected individual in a completely susceptible population. The next generation method is adopted to compute the basic reproduction number of typhoid sub-model. Consider the dynamics 2, let matrices  $\mathcal{F}_i$  represent the newly infected terms and  $\mathcal{V}_i$  the remaining terms given as

$$\mathcal{F}_i = \begin{bmatrix} \beta_T S_0 \left( \frac{\eta_1 A_T}{N} + \frac{B}{K} \right) \\ 0 \\ 0 \end{bmatrix} \quad \text{and } \mathcal{V}_i = \begin{bmatrix} (\sigma_1 + \mu)E_T \\ -\sigma_1 E_T + (\gamma_1 + \delta_1 + \mu)A_T \\ -\epsilon_1 A_T + \tau B \end{bmatrix}.$$

Therefore, the Jacobian matrices  $F$  and  $V$  at disease-free equilibrium is given as:

$$F = \begin{bmatrix} 0 & \frac{\beta_T S_0 \eta_1}{N} & \frac{\beta_T S_0}{K} \\ 0 & 0 & 0 \\ 0 & 0 & 0 \end{bmatrix}, \quad V = \begin{bmatrix} \sigma_1 + \mu & 0 & 0 \\ -\sigma_1 & \gamma_1 + \delta_1 + \mu & 0 \\ 0 & -\epsilon_1 & \tau \end{bmatrix}$$

Hence, the next generation matrix for this system is represented by  $FV^{-1}$  and the basic reproduction number is denoted by  $R_0^T = \rho(FV^{-1})$  where  $\rho$  is the spectral radius of next generation matrix  $FV^{-1}$  of the model obtained as:

$$R_0^T = \frac{\beta_T \sigma_1 \Lambda}{\mu(\sigma_1 + \mu)(\gamma_1 + \delta_1 + \mu)} \left( \frac{\eta_1}{N} + \frac{\epsilon_1}{K\tau} \right) \quad (12)$$

By interpretation,  $R_0^T$  denotes the average number of secondary typhoid cases produced by typhoid person at his or her effective infectious period at the time the person entered an entirely typhoid susceptible population. The typhoid virus model is governed by eight parameters which can predict the behavior of the system.

The local stability analysis of the disease-free equilibrium (DFE) for the system would be written in Jacobian form then evaluated at the DFE, then we shall identify the eigenvalues and connect the sign of the eigenvalues to the basic reproduction number ( $R_0^T$ ) already provided in equation 13, and finally state the stability condition.



Considering the state vector in the order:  $X = (S, E_T, A_T, B)$  and the disease-free equilibrium (no infection) is  $E_{0T} = (S_0 = \frac{\Lambda}{\mu}, 0, 0, 0)$ . (We assume a closed population with births balancing natural deaths then  $S_0 = N$ ). Linearizing the full 5D system around  $E_{0T}$  gives the Jacobian matrix  $J(E_{0T})$ .

In the variable order  $(S, E_T, A_T, B)$  it is

$$J(E_{DFE}) = \begin{pmatrix} -\mu & 0 & 0 & \beta_T \eta_1 & \beta_T \\ 0 & -\mu & 0 & \gamma_1 & 0 \\ 0 & 0 & -(\sigma_1 + \mu) & \beta_T \eta_1 & \beta_T \\ 0 & 0 & \sigma_1 & -(\gamma_1 + \delta_1 + \mu) & 0 \\ 0 & 0 & 0 & \varepsilon_1 & -\tau \end{pmatrix} \quad (13)$$

From the block structure, the top-left  $2 \times 2$  block is diagonal  $\text{diag}(-\mu, -\mu)$  and the lower-right  $3 \times 3$  block (is the infected subsystem) is:

$$J_1 = \begin{pmatrix} -(\sigma_1 + \mu) & \beta_T \eta_1 & \beta_T \\ \sigma_1 & -(\gamma_1 + \delta_1 + \mu) & 0 \\ 0 & \varepsilon_1 & -\tau \end{pmatrix} \quad (14)$$

It follows that from matrix 13 the two eigenvalues are  $\lambda_1 = -\mu$  and  $\lambda_2 = -\mu$  and from matrix 14, three eigenvalues gives a characteristics polynomial as

$$\chi_{J_1}(\lambda) = \det(\lambda I_3 - J_1) = \lambda^3 + a_1 \lambda^2 + a_2 \lambda + a_3 = 0 \quad (15)$$

According to Routh-Hurwitz stability conditions as found in Inayaturohmat et al, (2022). All roots of the cubic have negative real parts if only and if the following;  $a_1 > 0, a_3 > 0, a_1 a_2 > a_3$ .

### Endemic equilibrium point

The infection of typhoid fever is considered to persist in a given population which is usually described by the endemic equilibrium state (EEP). Consider  $E_1 = (S^*, E_T^*, A_T^*, R^*, B^*) > 0$  is the (EEP) for the system. Thus, rewriting equations 3 in endemic form as

$$S^* = \frac{\Lambda}{\lambda_T^* + \mu} \quad (16a)$$

$$E_T^* = \frac{\lambda_T^* S^*}{\sigma_1 + \mu} \quad (16b)$$

$$A_T^* = \frac{\sigma_1 E_T^*}{\gamma_1 + \delta_1 + \mu} \quad (16c)$$

$$R^* = \frac{\gamma_1 A_T^*}{\mu} \quad (16d)$$

$$B^* = \frac{\varepsilon_1 A_T^*}{\tau} \quad (16e)$$



Substituting equation 16b in 16c to  $A_T^* = \frac{\sigma_1 \lambda_T^* S^*}{(\sigma_1 + \mu)(\gamma_1 + \delta_1 + \mu)}$  and further define  $C = \frac{\sigma_1}{(\sigma_1 + \mu)(\gamma_1 + \delta_1 + \mu)}$  and replacing the value of  $S^*$  in equation 16a hence  $A_T^*$  becomes

$$A_T^* = \frac{C\Lambda\lambda_T^*}{\lambda_T^* + \mu} \tag{17}$$

Then solving these equations in terms of  $\lambda_T^*$  to have

$$a_0 A_T^{*2} + a_1 A_T^* + a_2 = 0 \tag{18}$$

where  $a_0 = \frac{\beta_T \eta_1 \epsilon_1}{N} > 0$ ,  $a_1 = \epsilon_1 \mu + \beta_T (\varphi_0 - C\Lambda\varphi_1)$  and

$$a_2 = K\tau\mu[1 - R_0^T] \tag{19}$$

It can be observed that  $a_0$  is always greater than zero and in the other hand  $a_2$  is negative when  $R_0^T > 1$ . Hence there exist a unique non-negative value for  $A_T^*$  and furthermore, a unique endemic point  $E_1$  if  $R_0^T > 1$ .

### Global Asymptotic Stability of Typhoid sub-model

Let us shall construct a Lyapunov function which depends on the infected compartment only to discuss the global stability of DFE of the model 10 and investigate the nature of its global stability.

**Theorem 3.1.3** If  $R_0^T < 1$ , the disease-free equilibrium point,  $E_0$  of model system 10 is asymptotically stable if  $R_0^T < 1$  and unstable if  $R_0^T > 1$

**Proof:** Considering the work of Abegye and Kpanja (2023), we define the Lyapunov function by considering equations 10 on the infected classes where  $a > 0, b > 0$  and  $c > 0$ , thus

$$L(E_T, A_T, B) = aE_T + bA_T + cB \tag{20}$$

For all  $t \geq 0, S(t) \leq S_0$  and  $\frac{dS}{dt} = \Lambda - (\lambda_T + \mu)S \leq \Lambda - \mu S$  and so  $S(t)$  cannot exceed  $S_0 = \frac{\Lambda}{\mu}$ .

Then differentiating equation 21 to have

$$\frac{dL}{dt} = a \frac{dE_T}{dt} + b \frac{dA_T}{dt} + c \frac{dB}{dt}$$

Choosing  $a, b, c$  so that  $E_T$  and  $B$  - coefficients are zero  $b = \frac{a(\sigma_1 + \mu)}{\sigma_1}, c = -\frac{a\beta_T S_0}{K\tau}$

It follows that

$$\frac{dL}{dt} \leq a \frac{(\sigma_1 + \mu)(\gamma_1 + \delta_1 + \mu)}{\sigma_1} (R_0^T - 1) \tag{21}$$

The Lyapunov function result for the Typhoid fever model is expressed as  $\frac{dL}{dt} \leq a \frac{(\sigma_1 + \mu)(\gamma_1 + \delta_1 + \mu)}{\sigma_1} (R_0^T - 1)$  where  $R_0^T$  denotes the basic reproduction number for Typhoid fever. This inequality shows that the evolution of the Lyapunov function



depends directly on whether  $R_0^T$  is less than or greater than one. If  $R_0^T < 1$  then,  $\frac{dL}{dt} \leq 0$ , meaning that the Lyapunov function decreases over time, which guarantees the global asymptotic stability of the disease-free equilibrium. This implies that the infection will die out from the population in the long run. Conversely, if  $R_0^T > 1$  then  $\frac{dL}{dt} > 0$ , showing that the Lyapunov function does not decrease, and the infection will persist, leading the system to an endemic state. Thus, the result emphasizes the threshold role of the basic reproduction number: Typhoid fever is eradicated when  $R_0^T < 1$ , while it persists in the population whenever  $R_0^T > 1$ .

### Sensitivity Analysis of Typhoid sub-model

Sensitivity analysis plays a crucial role in ascertaining the parameter that mostly influences the behaviour of  $\mathcal{R}_0$  which can easily aid in predicting in the intervention strategy of the dynamics. Relative changes can be measured in a variable when parameters vary noticeably in sensitivity indices. A parameter  $\Omega$  is considered to be sensitive when a small change in its parameter value gives a certain behavior to the model as in Nisar et al. (2024), described by

$$S_{\Omega}^{\mathcal{R}_0} = \frac{\partial \mathcal{R}_0}{\partial \Omega} \times \frac{\Omega}{\mathcal{R}_0} \quad (22)$$

The individual sensitivity index of the modeled parameters in  $\mathcal{R}_0^T$  are computed and the result shown below:

$$S_{\beta_T}^{\mathcal{R}_0^T} = +1, \quad S_{\sigma_1}^{\mathcal{R}_0^T} = \frac{\mu}{\sigma_1 + \mu}, \quad S_{\eta_1}^{\mathcal{R}_0^T} = \frac{\eta_1}{\eta_1 + \frac{\epsilon_1}{\tau}}, \quad S_{\epsilon_1}^{\mathcal{R}_0^T} = \frac{\epsilon_1}{\tau(\eta_1 + \frac{\epsilon_1}{\tau})}, \quad S_{\tau}^{\mathcal{R}_0^T} = -\frac{\tau}{\eta_1 + \frac{\epsilon_1}{\tau}}, \quad S_{\gamma_1}^{\mathcal{R}_0^T} = -\frac{\gamma_1}{\gamma_1 + \delta_1 + \mu},$$

$$S_{\delta_1}^{\mathcal{R}_0^T} = -\frac{\delta_1}{\gamma_1 + \delta_1 + \mu}, \quad S_{\mu}^{\mathcal{R}_0^T} = -\frac{(2\mu + \sigma_1 + \gamma_1 + \delta_1)}{(\sigma_1 + \mu)(\gamma_1 + \delta_1 + \mu)}$$

The sensitivity analysis shows that the basic reproduction number of typhoid,  $\mathcal{R}_0^T$ , responds most strongly to the transmission rate  $\beta_T$ , with a unit sensitivity, meaning that any increase in transmission directly raises disease spread. The progression rate from exposed to infectious ( $\sigma_1$ ), recovery with immunity ( $\eta_1$ ), and treatment failure ( $\epsilon_1$ ) also have positive sensitivities as found in Abdulai and Baba, (2023), indicating that faster incubation, more individuals returning to circulation, and failed treatments all contribute to sustaining transmission. On the other hand, treatment rate ( $\tau$ ), natural recovery ( $\gamma_1$ ), disease-induced death ( $\delta_1$ ), and natural death ( $\mu$ ) all have negative sensitivities, showing that increasing treatment coverage, improving recovery, or reducing the infectious period through removal of cases lowers  $\mathcal{R}_0^T$ . Thus, effective interventions should focus on reducing transmission  $\beta_T$ , expanding successful treatment ( $\tau$ ), and enhancing recovery ( $\gamma_1$ ), while minimizing treatment failures ( $\epsilon_1$ ), since these parameters exert the greatest influence on controlling typhoid spread.

### Hepatitis C Virus (HCV) only model

In absence of those infected by Typhoid fever (TF) by setting  $E_H = A_H = A_C = 0$ , then equations 3.39 – 3.46 becomes

$$\frac{dS}{dt} = \Lambda - (\lambda_H + \mu)S$$



$$\frac{dE_H}{dt} = \lambda_H S - (\sigma_2 + \mu)E_H$$

$$\frac{dA_H}{dt} = \sigma_2 E_H - (\gamma_2 + \delta_2 + \mu)A_H \quad (23)$$

$$\frac{dR}{dt} = \gamma_2 A_H - \mu R$$

$$\text{where } \lambda_H = \beta_H \frac{A_T}{N}$$

### The local stability of Hepatitis C Virus (HCV) sub-model

At  $A_H(t) = 0$  where there is no Hepatitis C Virus, we determinate the disease-free equilibrium point using equation 17 denoted by  $E_{0H} = \left(\frac{\Lambda}{\mu}, 0, 0, 0\right)$ . The basic reproduction number of the sub-model connotes the average number of secondary infections produced by a single Hepatitis C Virus infected individual in a completely susceptible population. The next generation method is adopted to compute the basic reproduction number of Hepatitis C Virus sub-model as in Daniel et al (2025). The matrix for the system are shown below as:

$$F = \begin{pmatrix} 0 & \beta_H \\ 0 & 0 \end{pmatrix} \quad \text{and} \quad V = \begin{pmatrix} \sigma_2 + \mu & 0 \\ -\sigma_2 & \gamma_2 + \delta_2 + \mu \end{pmatrix} \quad . \quad \text{Then} \quad \text{the} \quad V^{-1} = \begin{pmatrix} \frac{1}{\sigma_2 + \mu} & 0 \\ \frac{\sigma_2}{(\sigma_2 + \mu)(\gamma_2 + \delta_2 + \mu)} & \frac{1}{\gamma_2 + \delta_2 + \mu} \end{pmatrix}$$

It then follows that the largest spectrum radius gives the basic reproduction number of HCV is:

$$\rho(FV^{-1}) = R_0^H = \frac{\beta_H \sigma_2}{(\sigma_2 + \mu)(\gamma_2 + \delta_2 + \mu)} \quad (24)$$

By interpretation,  $R_0^H$  represent the average number of secondary typhoid cases produced by HCV person at his or her effective infectious period at the time the person entered an entirely typhoid susceptible population. The HCV model is governed by eight parameters which can predict the behavior of the system.

**Lemma 3.2.1** The disease-free equilibrium of the HCV sub-model is locally asymptotically stable (LAS) if threshold quantity is less than unity (Elaydi and Lozi, 2024).

In biological terms, for  $R_0^H < 1$  implies that the disease can easily be eradicated from the a given population (community) where it was initially pandemic. This is possible if the initial size of the sub-populations of the model is found in the basin of attraction of disease-free equilibrium (DFE). We use linearization approach to examine the local stability of HCV by considering the Jacobian matrix;  $J_{E_{0H}}$  and computing  $\det(J_{E_{0H}} - \lambda I)$  by expanding the 4<sup>th</sup> column (which entries are  $(0, 0, 0, -\mu - \lambda)$ ) hence,



$$\det(J_{E_{0H}} - \lambda I) = (-\mu - \lambda) \begin{pmatrix} -\mu - \lambda & 0 & -\frac{\beta_H S_0}{N} \\ 0 & -(\sigma_2 + \mu) - \lambda & \frac{\beta_H S_0}{N} \\ 0 & 0 & \sigma_2 - \lambda \end{pmatrix}$$

The  $3 \times 3$  matrix is upper-triangular, so its determinant is:  $(-\mu - \lambda)(-(\sigma_2 + \mu) - \lambda)(\sigma_2 - \lambda)$ . So, the eigenvalues are:  $\lambda_1 = \sigma_2, \lambda_2 = -(\sigma_2 + \mu), \lambda_3 = \lambda_4 = -\mu$

It can be seen that  $\lambda_2, \lambda_3$  and  $\lambda_4$  are strictly negative for any biologically realistic  $\mu > 0$  and  $\sigma_2 \geq 0$ . The stability hinge is  $\lambda_1 = \sigma_2$

If  $\sigma_2 > 0$  and  $\lambda_1 > 0$  One positive eigenvalue and the rest negative  $\Rightarrow$  the equilibrium is a saddle (unstable) a small perturbation along the  $\lambda_1$  direction grows, so the equilibrium is not asymptotically stable.

If  $\sigma_2 = 0$  and  $\lambda_1 = 0$  while the other three eigenvalues are negative implies the linearization is non-hyperbolic and linear analysis is inconclusive (you would need centre-manifold or higher-order terms to decide stability).

If  $\sigma_2 < 0$  would make all eigenvalues negative so the equilibrium would be asymptotically stable, but  $\sigma_2 < 0$  is usually not biologically meaningful since  $\sigma_2$  is a rate. Since  $\sigma_2$  is typically a transmission/progression rate  $\sigma_2 > 0$  means the infection can grow along that model, hence the disease-free (or studied) equilibrium is unstable unless you can drive the effective  $\sigma_2$  to zero (or negative, which isn't physical).

### The endemic equilibrium of HCV sub-model

In order to study the endemic equilibrium of HCV sub-model, we solve its ODEs by equating them to zeros and replacing  $S, E_H, A_H, R, \lambda_H$  with  $S^*, E_H^*, A_H^*, R^*$  and  $\lambda_H^*$ . Hence the equations are rewritten as:

$$S^* = \frac{\Lambda}{\lambda_H^* + \mu} \quad (25a)$$

$$E_H^* = \frac{\lambda_H^* \Lambda}{(\lambda_H^* + \mu)(\sigma_2 + \mu)} \quad (25b)$$

$$A_H^* = \frac{\lambda_H^* \Lambda \sigma_2}{(\lambda_H^* + \mu)(\sigma_2 + \mu)(\gamma_2 + \delta_2 + \mu)} \quad (25c)$$

$$R^* = \frac{\lambda_H^* \Lambda \sigma_2 \gamma_2}{\mu(\lambda_H^* + \mu)(\sigma_2 + \mu)(\gamma_2 + \delta_2 + \mu)} \quad (25d)$$

Given the force of infection,  $\lambda_H^* = \beta_H \frac{A_H^*}{N}$ . Then solving in terms of  $\lambda_H^*$  and simplifying to have

$$a_0 \lambda_H^{*2} + a_1 \lambda_H^* + a_2 = 0 \quad (26)$$

Where  $a_0 = 0$ ,  $a_1 = (\sigma_2 + \mu)(\gamma_2 + \delta_2 + \mu)$  and  $a_2 = 1 - R_0^H$



### Global Asymptotic Stability of HCV sub-model

We shall construct a Lyapunov function which depends on the infected compartment only to discuss the global stability of DFE of the model 24 and investigate its global stability nature.

**Theorem 3.2.3** If  $R_0^T < 1$ , the disease-free equilibrium point,  $E_{0H}$  of model system above is asymptotically stable if  $R_0^T < 1$  and unstable if  $R_0^T > 1$

**Proof:** Let us define the Lyapunov function as found in Abegye and Kpanja (2023) by considering equations HCV model on the infected classes where  $a > 0$  and  $b > 0$ , thus

$$L(E_H, A_H) = aE_H + bA_H \quad (27)$$

Differentiating equation 27 and choosing  $b = \frac{a(\sigma_2 + \mu)}{\sigma_2}$  in order to cancel  $E_H$ , then we have

$$\frac{dL}{dt} \leq aA_H \frac{(\sigma_2 + \mu)(\gamma_2 + \delta_2 + \mu)}{\sigma_2} [R_0^H - 1] \quad (28)$$

The result of the Lyapunov function for the HCV model shows that the time derivative  $\frac{dL}{dt}$  is bounded above by  $\frac{dL}{dt} \leq aA_H \frac{(\sigma_2 + \mu)(\gamma_2 + \delta_2 + \mu)}{\sigma_2} [R_0^H - 1]$  where  $A_H$  represents the population of individuals acutely infected with HCV, and  $R_0^H$  is the basic reproduction number of the infection. This inequality establishes that the sign of  $\frac{dL}{dt}$  is determined by whether  $R_0^H$  is less than one, or greater than one.

When  $R_0^H < 1$ , the derivative is non-positive, implying that the Lyapunov function decreases over time, and the disease-free equilibrium is globally asymptotically stable. On the other hand,  $R_0^H > 1$ , the derivative becomes positive, suggesting that the infection persists in the population and the system may move towards an endemic equilibrium. Therefore, the result highlights the threshold property of the reproduction number in governing the long-term dynamics of HCV: elimination of the disease is guaranteed when transmission potential is below the critical threshold, while persistence is inevitable if it exceeds that threshold.

### Sensitivity Analysis of HCV sub-model

The computation of the sensitivity indices of HCV is done as shown as in the previous section. The sensitivity indices of the five parameters follow accordingly;

$$S_{\beta_H}^{\mathcal{R}_0^H} = +1, S_{\sigma_2}^{\mathcal{R}_0^H} = \frac{\mu}{\gamma_2 + \delta_2 + \mu}, S_{\mu}^{\mathcal{R}_0^H} = -\frac{\mu(2\mu + \gamma_2 + \delta_2 + \sigma_2)}{(\sigma_2 + \mu)(\gamma_2 + \delta_2 + \mu)}, S_{\gamma_2}^{\mathcal{R}_0^H} = -\frac{\gamma_2}{\gamma_2 + \delta_2 + \mu}, S_{\delta_2}^{\mathcal{R}_0^H} = -\frac{\delta_2}{\gamma_2 + \delta_2 + \mu}$$

For  $S_{\beta_H}^{\mathcal{R}_0^H} = +1$  means that the basic reproduction number  $\mathcal{R}_0^H$  is directly proportional to the transmission rate of HCV. A sensitivity index of +1 indicates that a 1% increase in  $\beta_H$  will cause exactly a 1% increase in  $\mathcal{R}_0^H$  while a 1% decrease in  $\beta_H$  will result in a 1% decrease in  $\mathcal{R}_0^H$ . In other words,  $\mathcal{R}_0^H$  changes at the same rate as  $\beta_H$ . This shows that the transmission rate is a highly influential parameter in determining the spread of HCV, and effective control measures should therefore focus on reducing  $\beta_H$  (for example, through safe injection practices, blood screening, and awareness campaigns), since any reduction directly lowers the reproduction number and hence the potential for sustained transmission.



Also,  $S_{\sigma_2}^{\mathcal{R}_0^H} = \frac{\mu}{\gamma_2 + \delta_2 + \mu}$ , the expression has a clear biological interpretation. The index is still positive, meaning that an increase in the progression rate  $\sigma_2$  (the rate at which exposed individuals progress to the acute infectious stage) leads to an increase in  $\mathcal{R}_0^H$ . However, the effect is not one-to-one as with the transmission rate; instead, the influence is scaled by the fraction  $\frac{\mu}{\gamma_2 + \delta_2 + \mu}$ . Since  $\mu$  (natural death) is usually small compared to  $(\gamma_2 + \delta_2 + \mu)$  the sensitivity value is less than 1, often quite small. This indicates that while  $\sigma_2$  contributes to the spread of HCV, its relative impact on  $\mathcal{R}_0^T$  is weaker compared to parameters like  $\beta_H$ .

Biologically, it implies that increasing the rate at which exposed individuals become acutely infected only moderately affects disease transmission, because recovery, disease-induced death, and natural death counterbalance this progression.

In the case of  $S_{\mu}^{\mathcal{R}_0^H}$  this negative sign means that increasing the natural death rate  $\mu$  decreases the basic reproduction number  $\mathcal{R}_0^H$  a small percentage increase in  $\mu$  produces a percentage decrease in  $\mathcal{R}_0^H$  given by the value of the index. The factor  $\frac{\mu(2\mu + \gamma_2 + \delta_2 + \sigma_2)}{(\sigma_2 + \mu)(\gamma_2 + \delta_2 + \mu)}$  quantifies the strength of that effect; because every term in the numerator and denominator is positive, the index is strictly negative for biologically meaningful parameter values. In practical, biological terms this reflects that larger rates of removal from the population (natural mortality) shorten the average time individuals can contribute to transmission, thus reducing  $\mathcal{R}_0^H$ .

Similarly,  $S_{\gamma_2}^{\mathcal{R}_0^H}$ , shows a negative index, an increase in the recovery rate  $\gamma_2$  produces a proportional decrease in the basic reproduction number  $\mathcal{R}_0^H$ : this implies that a 1% increase in  $\gamma_2$  yields approximately a  $\frac{\gamma_2}{\gamma_2 + \delta_2 + \mu}$  % decrease in  $\mathcal{R}_0^H$ . The magnitude  $\frac{\gamma_2}{\gamma_2 + \delta_2 + \mu}$  lies between 0 and 1, so the effect is always reducing but typically smaller than a one-to-one change. Biologically this makes sense: faster recovery shortens infectiousness and therefore lowers transmission potential. Practically, this shows that interventions which increase the recovery rate (improved treatment, faster case detection and care) are effective levers for lowering  $\mathcal{R}_0^H$ .

In the case of  $S_{\delta_2}^{\mathcal{R}_0^H}$ , the result means that as the disease-induced death rate of chronic HCV patients ( $\delta_2$ ) increases, the basic reproduction number  $\mathcal{R}_0^H$  decreases, thereby reducing the potential for the disease to spread.

### The impact of Typhoid fever on HCV

With a careful search on the two  $\mathcal{R}_0^H$  and  $\mathcal{R}_0^T$  there is no direct impact since  $\mathcal{R}_0^H$  does not depend on any typhoid parameter therefore there is no direct effect of typhoid on HCV. However, typhoid can affect HCV *indirectly* through shared demography or shared model parameters (for example the death rate  $\mu$ , total population  $N$ , or rates that change because of health-system strain). The algebra for those indirect pathways is shown below by the use of a compact chain-rule relation assuming typhoid acts only by changing  $\mu$ . This ideal was borrowed from adopting Elasticity (normalized sensitivity) to  $\mu$ .

Take logs and differentiate to get the elasticity of  $S_{\mu}^{\mathcal{R}_0^H}$ :



$$S_{\mu}^{\mathcal{R}_0^H} = -\frac{\mu}{\sigma_2 + \mu} - \frac{\mu}{\gamma_2 + \delta_2 + \mu}$$

In a similar way if  $D = \beta_T \sigma_1 \left( \frac{K\tau\eta_1}{N} + \epsilon_1 \right)$  as a constant in  $\mathcal{R}_0^T$  then,

$$\mathcal{R}_0^T = \frac{D}{\mu(\sigma_1 + \mu)(\gamma_1 + \delta_1 + \mu)} \Rightarrow S_{\mu}^{\mathcal{R}_0^T} = \frac{\partial \mathcal{R}_0^T}{\partial \mu} \times \frac{\mu}{\mathcal{R}_0^T} = -\left( 1 + \frac{\mu}{\sigma_2 + \mu} + \frac{\mu}{\gamma_2 + \delta_2 + \mu} \right)$$

Interpretation of both elasticities are negative (increasing  $\mu$  reduces both reproduction numbers).

### Computation of the threshold quantity of the co-infection

We use the next-generation method (van den Driessche and Watmough) as found in Konlan (2024). Taking the infected-state vector as  $= (S, E_T, A_T, E_H, A_H, A_C, B)^T$ . At the disease-free equilibrium (DFE) all infected variables are zero and  $S_0 = N_0 = \frac{\Lambda}{\mu}$ . The system is linearizing  $\frac{B}{K+B}$  near  $B \approx 0$  by  $\frac{B}{K+B} \approx \frac{B}{K}$ . The within-linearized forces of infection at the DFE are  $\lambda_T = \beta_T \left( \frac{\eta_1 A_T + \eta_2 A_C}{N} + \frac{B}{K+B} \right)$  and  $\lambda_H = \beta_H \left( \frac{A_H + A_C}{N} \right)$ . Since  $\frac{S_0}{N_0} = 1$  the new-infection terms simplify accordingly.

$$F = \begin{pmatrix} 0 & \beta_T \eta_1 & 0 & 0 & \beta_T \eta_2 & \beta_T \frac{S_0}{K} \\ 0 & 0 & 0 & 0 & 0 & 0 \\ 0 & 0 & 0 & \beta_H & \beta_H & 0 \\ 0 & 0 & 0 & 0 & 0 & 0 \\ 0 & 0 & 0 & 0 & 0 & 0 \\ 0 & 0 & 0 & 0 & 0 & 0 \end{pmatrix}, \quad V = \begin{pmatrix} A_1 & 0 & 0 & 0 & 0 & 0 \\ -\sigma_1 & A_2 & 0 & 0 & -\theta_1 & 0 \\ 0 & 0 & A_3 & 0 & 0 & 0 \\ 0 & 0 & -\sigma_2 & A_4 & -\theta_2 & 0 \\ 0 & 0 & 0 & 0 & \gamma_5 & 0 \\ 0 & -\epsilon_1 & 0 & 0 & -\epsilon_2 & \tau \end{pmatrix}$$

For  $A_1 = \sigma_1 + \mu, A_2 = \gamma_1 + \delta_1 + \mu, A_3 = \sigma_2 + \mu, A_4 = \gamma_2 + \delta_2 + \mu, A_5 = \gamma_3 + \theta_1 + \theta_2 + \delta_3 + \mu$ .

The computation of  $V^{-1}$  is carried out by solving  $Vx = e_j$  for  $j = 1, \dots, 6$  as used by Nisar et al, (2024).

The algebra is done for each obtained and the result follows accordingly below:



$$V^{-1} = \begin{pmatrix} \frac{1}{A_1} & 0 & 0 & 0 & 0 & 0 \\ \frac{\sigma_1}{A_1 A_2} & \frac{1}{A_2} & 0 & 0 & \frac{\theta_1}{A_2 A_5} & 0 \\ 0 & 0 & \frac{1}{A_3} & 0 & 0 & 0 \\ 0 & 0 & \frac{\sigma_2}{A_3 A_4} & \frac{1}{A_4} & \frac{\theta_2}{A_4 A_5} & 0 \\ 0 & 0 & 0 & 0 & \frac{1}{A_5} & 0 \\ \frac{\varepsilon_1 \sigma_1}{A_1 A_2 \tau} & \frac{\varepsilon_1}{A_2 \tau} & 0 & 0 & \frac{\varepsilon_1 \theta_1 + A_2 \varepsilon_2}{A_1 A_2 \tau} & \frac{1}{\tau} \end{pmatrix}$$

Matrix F has only two nonzero rows (row 1 for new typhoid infections, row 3 for new infections)

$F_{1,2} = \beta_T \eta_1, F_{1,5} = \beta_T \eta_2, F_{1,6} = \beta_T \frac{S_0}{K}, F_{3,4} = \beta_H, F_{3,5} = \beta_H$  all other  $F_{i,j} = 0$ . Using the  $V^{-1}$  derived previously the product  $K = FV^{-1}$  has nonzero only in row 1 and row 3. Adopting the processes used by Thierry et al, (2025), matrix K is given by:

$$K = \begin{pmatrix} K_{1,1} & K_{1,2} & 0 & 0 & K_{1,5} & K_{1,6} \\ 0 & 0 & 0 & 0 & 0 & 0 \\ 0 & 0 & K_{3,3} & K_{3,4} & K_{3,5} & 0 \\ 0 & 0 & 0 & 0 & 0 & 0 \\ 0 & 0 & 0 & 0 & 0 & 0 \\ 0 & 0 & 0 & 0 & 0 & 0 \end{pmatrix}$$

where  $K_1$  and  $K_3$  are given below. The HCV contribution appears as:

$$R_0^H = \frac{\beta_H \sigma_2}{(\sigma_2 + \mu)(\gamma_2 + \delta_2 + \mu)} \tag{29}$$

The Typhoid contribution equals the dominant-eigenvalue coming from the typhoid generated from the sub-block given by

$$R_0^T = \frac{\beta_T \sigma_1}{(\sigma_1 + \mu)(\gamma_1 + \delta_1 + \mu)} \left( \eta_1 + \frac{S_0 \varepsilon_1}{K \tau} \right) \tag{30}$$

Hence the spectral radius (basic reproduction number) of the co-infection of K is



$$\mathcal{R}_0 = \max\{R_0^T, R_0^H\} \tag{31}$$

### The local stability of HCV-typhoid co-infection model

Linearization method was used to investigate the stability of the disease-free equilibrium point for the co-infection of HCV-typhoid co-infect model which is analysed as follows. The Jacobian matrix of the co-infection from equation 2 is shown below:

$$J_{E_0^{HT}} = \begin{bmatrix} -\mu & 0 & -\beta_T \eta_1 & 0 & -\beta_H & -(\beta_T \eta_1 + \beta_H) & 0 & -\frac{S_0 \beta_T}{K} \\ 0 & -(\sigma_1 + \mu) & \beta_T \eta_1 & 0 & 0 & \beta_T \eta_2 & 0 & \frac{S_0 \beta_T}{K} \\ 0 & \sigma_1 & -(\gamma_1 + \delta_1 + \mu) & 0 & 0 & \theta_1 & 0 & 0 \\ 0 & 0 & 0 & -(\sigma_2 + \mu) & \beta_H & \beta_H & 0 & 0 \\ 0 & 0 & 0 & \sigma_2 & -(\gamma_2 + \delta_2 + \mu) & \theta_2 & 0 & 0 \\ 0 & 0 & 0 & 0 & 0 & -(\gamma_3 + \theta_1 + \theta_2 + \delta_3 + \mu) & 0 & 0 \\ 0 & 0 & \gamma_1 & 0 & \gamma_2 & \gamma_3 & -\mu & 0 \\ 0 & 0 & \varepsilon_1 & 0 & 0 & \varepsilon_2 & 0 & -\tau \end{bmatrix}$$

**Lemma 4.1** If  $R_0^H < 1$  and  $R_0^T < 1$  at disease-free equilibrium then the system is locally asymptotically stable (LAS) and if  $R_0^H > 1$  and  $R_0^T > 1$ , then it is unstable.

Adopting block structure strategy as used by Joshua, Akpan and Inyang (2024) to obtain the eigenvalues of model as used by Singh et al, (2023). By reordering the system so the infected subsystem vector is  $(E_T, A_T, E_H, A_H, A_C, B)$  which gives a  $6 \times 6$  block and the uninfected states  $S, R$  form the remaining  $2 \times 2$  block. Because the infected block does not depend on  $S$  or  $R$  at the linearized level (their derivatives w.r.t.  $S, R$  evaluate to zero at DFE), the Jacobian is block-lower triangular of the form  $J_{E_0^{HT}} = \begin{pmatrix} M & 0 \\ C & D \end{pmatrix}$ ; hence the spectrum of  $J$  is the union of the spectra of the infected block  $M$  and of  $D$  (the  $S, R$  diagonal block). From the  $S, R$  diagonal entries we immediately get two eigenvalues:  $\lambda_1 = -\mu, \lambda_2 = -\mu$ .

Now we analyse the infected  $6 \times 6$  block, using the same ordering  $(E_T, A_T, E_H, A_H, A_C, B)$  is:

$$J_{E_0^{HT}} = \begin{pmatrix} -(\sigma_1 + \mu) & \beta_T \eta_1 & 0 & 0 & \beta_T \eta_2 & \frac{\beta_T \Lambda}{K \mu} \\ \sigma_1 & -(\gamma_1 + \delta_1 + \mu) & 0 & 0 & \theta_1 & 0 \\ 0 & 0 & -(\sigma_2 + \mu) & \beta_H & \beta_H & 0 \\ 0 & 0 & \sigma_2 & -(\gamma_2 + \delta_2 + \mu) & \theta_2 & 0 \\ 0 & 0 & 0 & 0 & -(\gamma_3 + \theta_1 + \theta_2 + \delta_3 + \mu) & 0 \\ 0 & \varepsilon_1 & 0 & 0 & \varepsilon_2 & -\tau \end{pmatrix}$$



It can be observed that row 5 ( $A_C$ ) has only the diagonal entry  $-(\gamma_3 + \theta_1 + \theta_2 + \delta_3 + \mu)$ ; expanding the characteristic determinant along that row shows that;

$$\lambda_1^{A_C} = -(\gamma_3 + \theta_1 + \theta_2 + \delta_3 + \mu)$$

is an eigenvalue of  $J_{E_{02}^{HT}}$ .

After factoring that eigenvalue out, the remaining eigenvalues come from the reduced  $5 \times 5$  minor (indices  $(E_T, A_T, E_H, A_H, A_C, B)$ ), which actually decomposes into a decoupled HCV  $2 \times 2$  block and a typhoid/environmental  $3 \times 3$  block.

Hence for HCV  $2 \times 2$  sub-block  $(E_H, A_H)$

$$J_{E_{03}^{HT}} = \begin{pmatrix} -(\sigma_2 + \mu) & \beta_H \\ \sigma_2 & -(\gamma_2 + \delta_2 + \mu) \end{pmatrix}$$

Hence the characteristic equation is:

$$\lambda^2 + [(\sigma_2 + \mu) + (\gamma_2 + \delta_2 + \mu)]\lambda + (\sigma_2 + \mu)(\gamma_2 + \delta_2 + \mu) - \beta_H\sigma_2 = 0$$

So, the two eigenvalues are:

$$\lambda_{3,4}^2 = - \left[ \frac{(\sigma_2 + \mu)(\gamma_2 + \delta_2 + \mu)}{2} \right] \pm \frac{1}{2} \sqrt{((\sigma_2 + \mu) - (\gamma_2 + \delta_2 + \mu))^2 + 4\beta_H\sigma_2}$$

The HCV subblock is locally stable (both eigenvalues negative) iff

$$(\sigma_2 + \mu)(\gamma_2 + \delta_2 + \mu) - \beta_H\sigma_2 > 0$$

That is  $\beta_H\sigma_2 < (\sigma_2 + \mu)(\gamma_2 + \delta_2 + \mu)$ , which means  $\frac{\beta_H\sigma_2}{(\sigma_2 + \mu)(\gamma_2 + \delta_2 + \mu)} < 1 = R_0^H < 1$

Also, for Typhoid and Environmental sub-block  $3 \times 3(E_T, A_T, B)$

Ordering  $(E_T, A_T, B)$ , the  $3 \times 3$  matrix is:

$$J_{E_{04}^{HT}} = \begin{pmatrix} -(\sigma_1 + \mu) & -\beta_T\eta_1 & \frac{\beta_T\Lambda}{K\mu} \\ \sigma_1 & -(\gamma_1 + \delta_1 + \mu) & 0 \\ 0 & \epsilon_1 & -\tau \end{pmatrix}$$

Its characteristic polynomial (set  $\lambda$  as eigenvalue) can be written compactly as

$$(\lambda + \tau)[(\lambda + (\sigma_1 + \mu))(\lambda + (\gamma_1 + \delta_1 + \mu)) - \beta_T\eta_1\sigma_1] - \left(\frac{\beta_T\Lambda}{K\mu}\right)\sigma_1\epsilon_1 = 0$$

This is equivalent to:

$$(\lambda + \tau)[(\lambda + a)(\lambda + b) - \beta_T\eta_1\sigma_1] - c\sigma_1\epsilon_1 = 0$$

where  $a = \sigma_1 + \mu$ ,  $b = \gamma_1 + \delta_1 + \mu$ ,  $c = \frac{\beta_T\Lambda}{K\mu}$  This is a cubic in  $\lambda$  written as



$$\lambda^3 + (a + g + \tau)\lambda^2 + (ag + \tau(a + g) - \beta_T\eta_1\sigma_1)\lambda + ag\tau - \beta_T\eta_1\sigma_1 - c\sigma_1\epsilon_1 = 0$$

Now with the polynomial:  $\lambda^3 + b_1\lambda^2 + b_2\lambda + b_3 = 0$

Where  $b_1 = a + g + \tau$ ,  $b_2 = ag + \tau(a + g) - \beta_T\eta_1\sigma_1$ ,  $b_3 = ag\tau - \beta_T\eta_1\sigma_1 - c\sigma_1\epsilon_1$

Using Routh–Hurwitz Criterion, the three eigenvalues are negative if  $b_1 > 0$ ,  $b_3 > 0$  and

$$b_1b_2 > b_3$$

Indeed,  $b_1 > 0$  Since the parameters are biological rates, they are usually positive, so this is typically satisfied.

$b_3 > 0$ , which implies  $ag\tau - \beta_T\eta_1\sigma_1 - c\sigma_1\epsilon_1 > 0$

### Interpretation:

The product  $ag\tau$  (decay / removal-type terms) must dominate the two terms that decrease  $b_3$ : the transmission-like term  $\beta_T\eta_1\sigma_1$  and the extra loss  $c\sigma_1\epsilon_1$  there is at least one root with non-negative real part (instability or marginal stability).

Then for  $b_1b_2 > b_3 \Rightarrow (a + g + \tau)(ag + \tau(a + g) - \beta_T\eta_1\sigma_1) > (ag\tau - \beta_T\eta_1\sigma_1 - c\sigma_1\epsilon_1)$

This inequality prevents sign changes in the first column caused by the middle row; it couples the second-order coefficient  $b_2$  to  $b_3$ . If it fails you get a sign change in the Routh array and therefore at least one root with non-negative real part.

### The endemic state of HCV-typhoid co-infection model

The endemic and equilibrium point is the steady state solution in which the disease persist and affect the given population which can be denoted by  $E_0^* = (S^*, E_T^*, A_T^*, E_H^*, A_H^*, A_C^*, R, B)$ .

The endemic state was obtained by setting all the differential equations from the model (3) to zero and then solving for all compartments. We obtained two equilibria of the model, namely, disease-free equilibrium and endemic equilibrium denoted by  $E_0$  and  $E_0^*$  respectively. Denoting

$S = S^*$ ,  $E_T = E_T^*$ ,  $A_T = A_T^*$ ,  $E_H = E_H^*$ ,  $A_H = A_H^*$ ,  $A_C = A_C^*$ ,  $R = R^*$ ,  $B = B^*$ ,  $\lambda_T = \lambda_T^*$  and  $\lambda_H = \lambda_H^*$ . Where

$$b_1 = \sigma_1 + \mu, b_2 = \gamma_1 + \delta_1 + \mu, b_3 = \sigma_2 + \mu, b_4 = \gamma_2 + \delta_2 + \mu, b_5 = \gamma_3 + \theta_1 + \theta_2 + \delta_3 + \mu.$$

Therefore, solving for the variables from equations 3, to get

$$S^* = \frac{\Lambda}{\lambda_H^* + \lambda_T^* + \mu}$$

$$E_T^* = \frac{\lambda_T^* S^*}{b_1}$$

$$A_T^* = \frac{\sigma_1 E_T^* + \theta_1 A_C^*}{\lambda_H^* + b_2}$$



$$\begin{aligned}
 E_H^* &= \frac{\lambda_H S^*}{b_3} \\
 A_H^* &= \frac{\sigma_2 E_H^* + \theta_2 A_C^*}{\lambda_T + b_4} \quad (32) \\
 A_C^* &= \frac{\lambda_H A_T^* + \lambda_T A_H^*}{b_5} \\
 R^* &= \frac{\gamma_1 A_T^* + \gamma_2 A_H^* + \gamma_3 A_C^*}{\mu} \\
 B^* &= \frac{\epsilon_1 A_T^* + \epsilon_2 A_C^*}{\tau}
 \end{aligned}$$

### Global stability of HCV-typhoid co-infection model

Taking the standard log-type of Lyapunov function centred at the positive equilibrium  $x^*$  as in Joshua, Akpan and Inyang, (2024). Define,

$$V(x) = \sum \left( x_i - x_i^* - x_i^* \ln \frac{x_i}{x_i^*} \right) \quad (33)$$

Where the sum runs over  $x_i \in \{S, E_T, A_T, E_H, A_H, A_C, R, B\}$ . The Lyapunov function has the following properties:

- (i)  $V(x) \geq 0$  for all  $x > 0$  and
- (ii)  $V(x) = 0$  iff  $x = x^*$  for every compartment as found in Elaydi and Lozi, (2024).

**Theorem 4.3** The disease was considered to exist at equilibrium point if  $R_0^T > 1, R_0^H > 1$  and said to be globally stable (Avendano et al, 2002).

**Proof:** Differentiating along trajectories with the identity of the Lyapunov function of equation 3.126 is given as

$$\dot{V}(x) = \sum_x \left( 1 - \frac{x^*}{x} \right) \dot{x}$$

In computing each compartment contribution, we substitute each  $\dot{x}$  for each compartment and use the equilibrium relation  $\dot{x} = 0$  to rewrite the differences, we have

$$\begin{aligned}
 \dot{V}(x) = & \\
 & -\mu \left( \frac{S - S^*}{S} \right)^2 - b_1 \left( \frac{E_T - E_T^*}{E_T} \right)^2 - b_2 \left( \frac{A_T - A_T^*}{A_T} \right)^2 - b_3 \left( \frac{E_H - E_H^*}{E_H} \right)^2 \\
 & - b_4 \left( \frac{A_H - A_H^*}{A_H} \right)^2 - b_5 \left( \frac{A_C - A_C^*}{A_C} \right)^2 - \mu \left( \frac{R - R^*}{R} \right)^2 - \tau \left( \frac{B - B^*}{B} \right)^2 + C \quad (34)
 \end{aligned}$$

Where C collects the remaining terms coupling terms (those including  $\lambda_T S - \lambda_T^* S^*, \lambda_H S - \lambda_H^* S^*, \sigma_1, \theta_1, \gamma_1, \epsilon_1$  linear cross terms, etc).

Next, we expand and compute the difference of force infection as follows:



$$\begin{aligned}\lambda_T - \lambda_T^* &= \beta_T \left( \frac{\eta_1(A_T - A_T^*) + \eta_2(A_C - A_C^*)}{N} + \frac{B}{K+B} - \frac{B^*}{K+B^*} \right) \\ &= \beta_T \left( \frac{\eta_1(A_T - A_T^*) + \eta_2(A_C - A_C^*)}{N} + \frac{K(B - B^*)}{(K+B)(K+B^*)} \right)\end{aligned}\quad (35)$$

And

$$\lambda_H - \lambda_H^* = \beta_T \left( \frac{(A_H - A_H^*) + (A_C - A_C^*)}{N} \right)\quad (36)$$

Both differences are defined (linear) combinations of  $A_T - A_T^*$ ,  $A_H - A_H^*$ ,  $A_C - A_C^*$ ,  $B - B^*$ . That is crucial, every  $\lambda -$  differences become a linear combination of the same compartment difference that appear elsewhere.

The coupling C is considered as follows: Look at one typical pair of terms involving  $\lambda_H S$  forms  $S$  &  $E_T$  terms we had the combination

$$-\left(1 - \frac{S^*}{S}\right)(\lambda_T S - \lambda_T^* S^*) + \left(1 - \frac{E_T^*}{E_T}\right)(\lambda_T S - \lambda_T^* S^*)$$

Factoring  $(\lambda_T S - \lambda_T^* S^*)$  which gives  $\left(\frac{S^*}{S} - \frac{E_T^*}{E_T}\right)$ , then rewriting

$$\lambda_T S - \lambda_T^* S^* = \lambda_T(S - S^*) + S^*(\lambda_T - \lambda_T^*)$$

So, the multiplier splits the combination into two types that is terms proportion to  $\lambda_T(S - S^*)$ , these pairs with similar terms coming from

$$\dot{V}(x) = - \sum C_i \frac{(x_i - x^*)^2}{x} \leq 0 \quad (37)$$

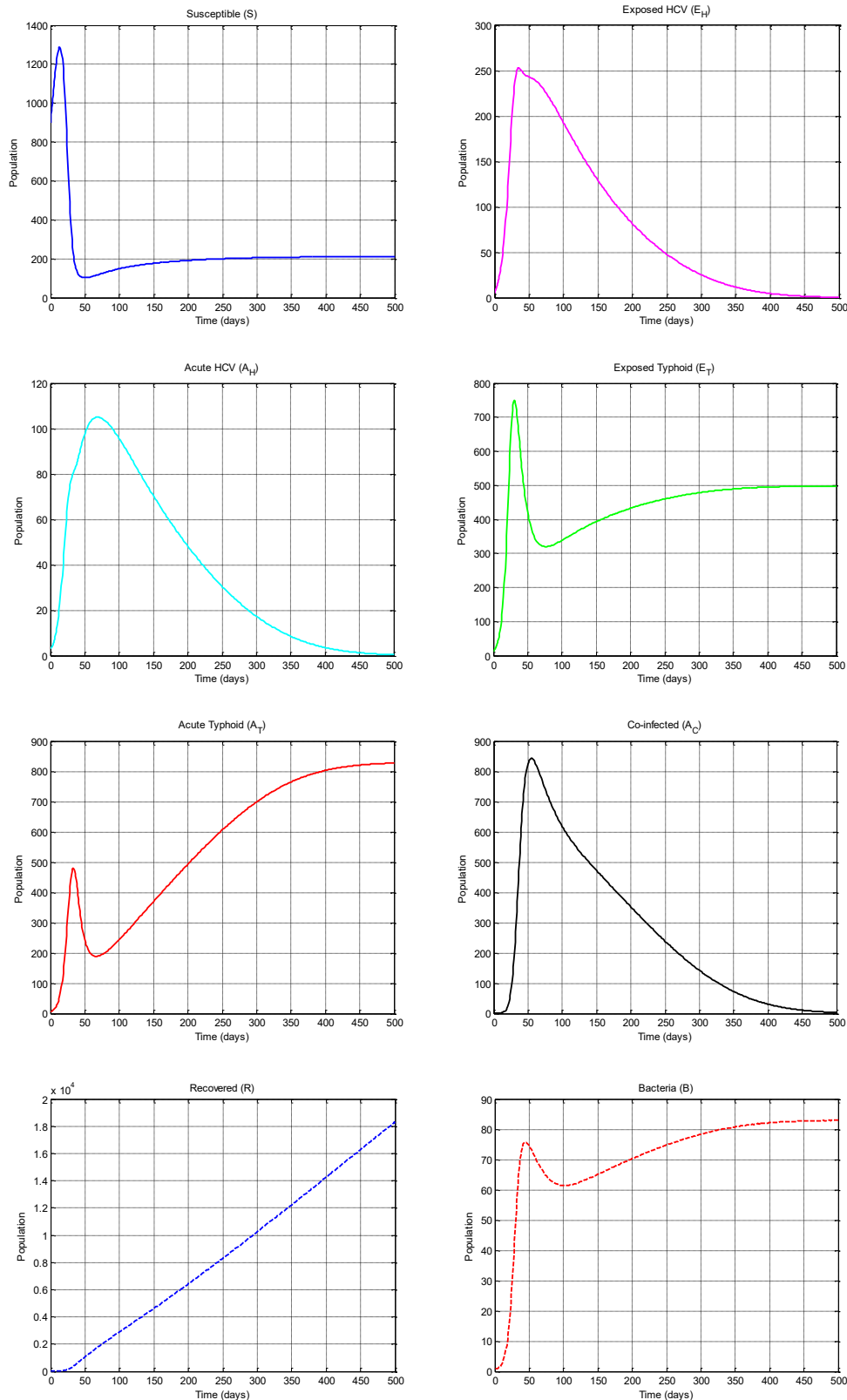
Where each  $C_i > 0$  is a combination of the model parameters  $\mu, b_1, \dots, b_5, \gamma_i, \tau, \beta_T, \beta_H$ , etc. In particular,  $\dot{V} < 0$  for all positive states and  $\dot{V} = 0 \Leftrightarrow x = x^*$ , the positive endemic equilibrium  $x^*$  is globally asymptotically stable in the positive orthant. Hence the prove established.

## NUMERICAL SIMULATION AND DISCUSSION OF RESULTS

In this section, the study aim at verifying some of the analytical results obtained above both for the sub-model and the co-infection models and compares these results with the numerical results. This is achieved by using the values of the parameters obtained from literatures shown in table 8. The simulation is done using MATLAB ODE solver.

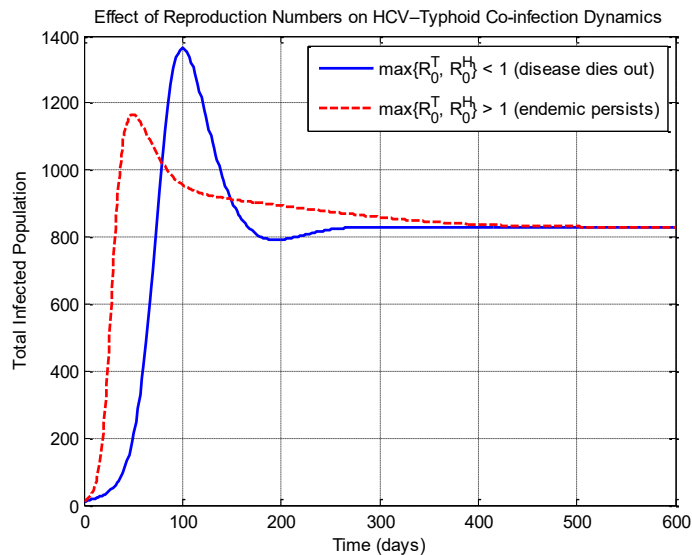
**Plots showing behavior of each population of the model**

**Figure 1: The plots shows the behavior individual compartments.**



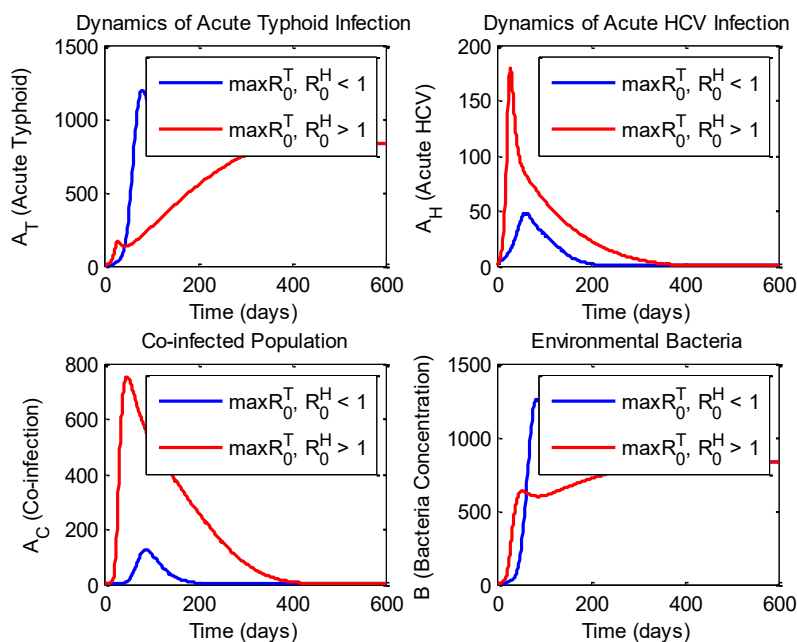
**Plots showing the effect of basic reproduction number on the model**

**Figure 2: The plot shows both curves on the same axes where blue line indicate infection fades (below threshold) and red dashed line represent infection persists (above threshold)**



**Plots comparing the dynamics on infections**

**Figure 3: The plots compare  $R_0^T, R_0^H$  scenarios on acute typhoid, acute HCV, co-infection and bacterial with low ( $\beta_T = \beta_H = 0.2$ ) and high ( $\beta_T = 0.8, \beta_H = 0.9$ ) transmissions**



### Plots showing parameter Sensitivity Analysis

Now let's explore the parameter sensitivity of HCV-typhoid co-infection model using four plots. Each plot shows how changing a key parameter (by  $\pm 30\%$ ) affects the total infected populations  $A_T + A_H + A_C$ , which gives the overall infection burden in the community.

**Figure 4: Sensitivity to  $\beta_T$  (Typhoid transmission rate), parameter varied  $\beta_T = 0.5 \times (0.7, 1.0, 1.3)$**

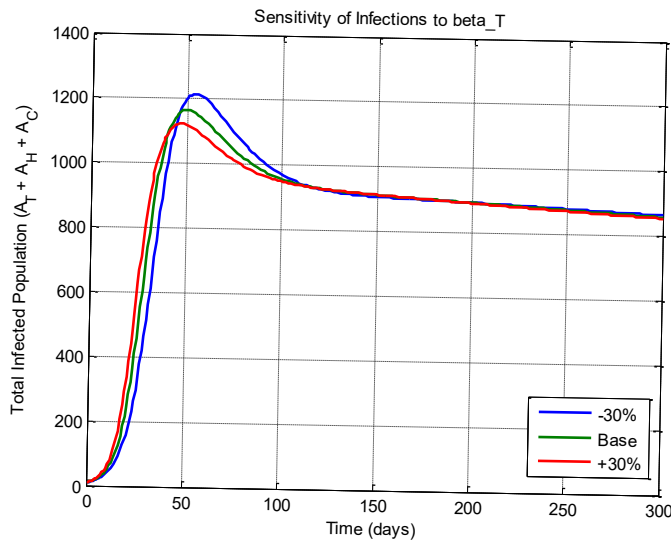


**Figure 5: Sensitivity to  $\beta_H$  (HCV transmission rate), parameter varied  $\beta_H = 0.6 \times (0.7, 1.0, 1.3)$**

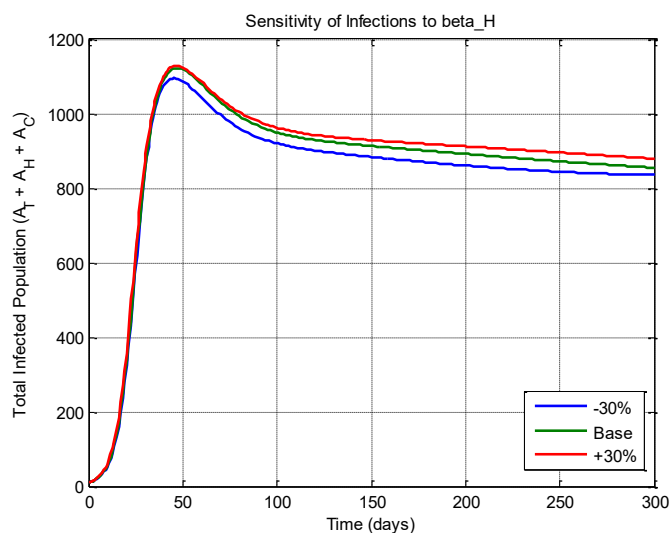


**Figure 6: Sensitivity to  $\gamma_1$  (Typhoid recovery rate), parameter varied  $\gamma_1 = 0.05 \times (0.7, 1.0, 1.3)$**

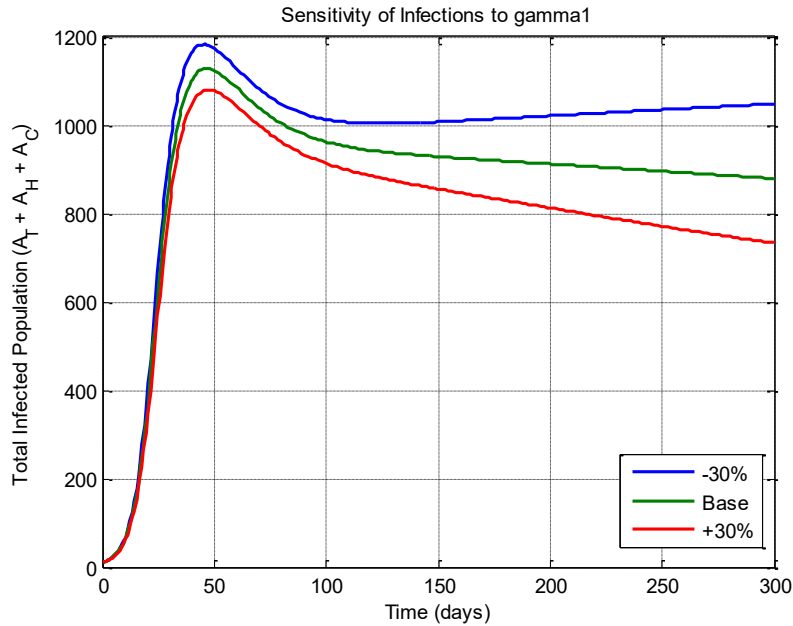


**Figure 7: Sensitivity to  $\gamma_2$  (HCV recovery rate), parameter varied  $\gamma_2 = 0.04 \times (0.7, 1.0, 1.3)$**

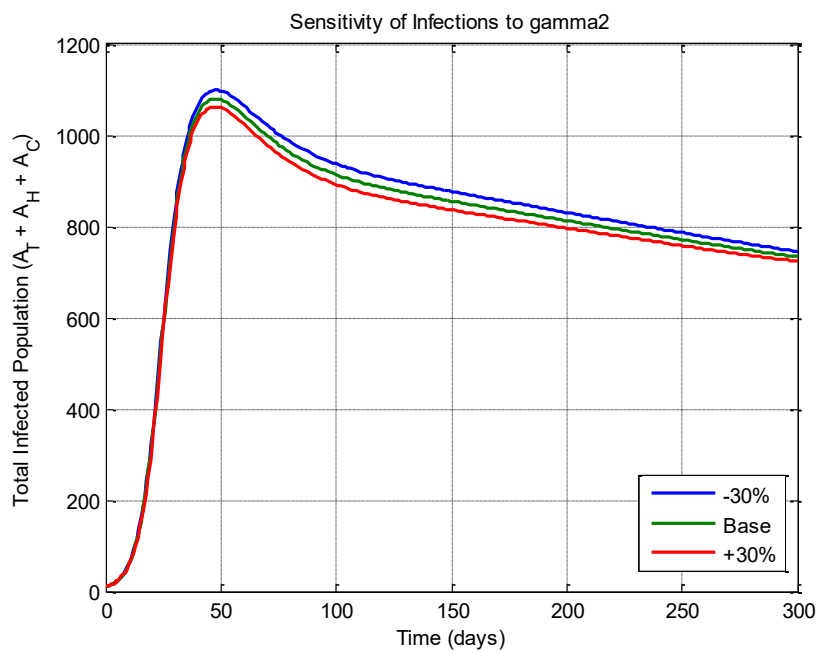


**Figure 8: Sensitivity to  $\tau$  (Environmental clearance rate), parameter varied  $\tau = 0.5 \times (0.7, 1.0, 1.3)$**

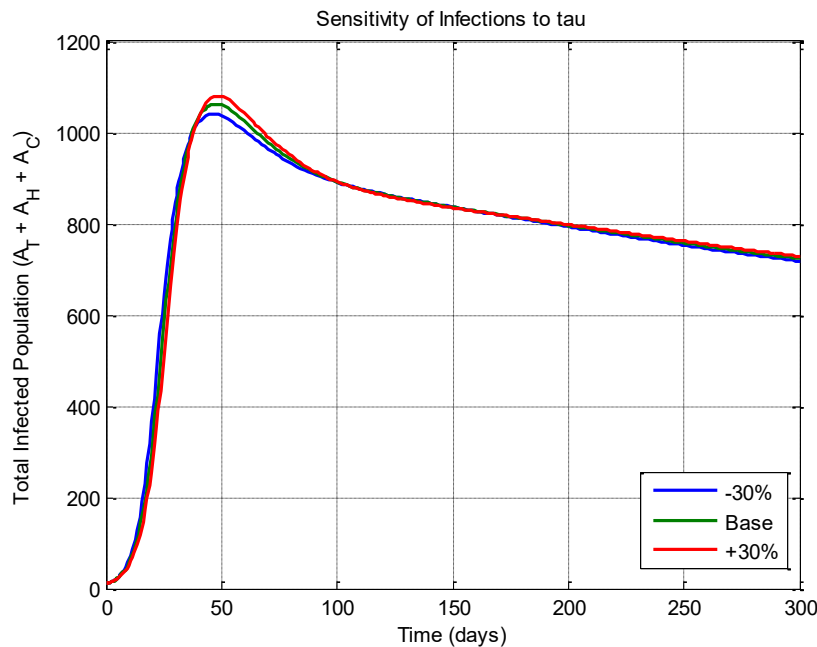


Figure 1 shows the behavior of each population accordingly. The susceptible population begins at a high level due to continuous recruitment and low natural death. Over time, exposure to Typhoid and HCV reduces the susceptible class until it stabilizes at an equilibrium level. The exposed Typhoid class rises rapidly in the early stage due to infection from infectious individuals and environmental bacteria. It peaks early and then declines as individuals progress to the acute stage and the system approaches equilibrium. The acute Typhoid population increases after exposure and later stabilizes as recovery, death, and transition to co-infection reduce the number of infectious individuals. The exposed HCV population grows more slowly due to a lower incubation rate and fewer initial infections, eventually stabilizing as the system approaches equilibrium. The acute HCV class shows a delayed and smoother increase compared to Typhoid, reflecting longer infectious periods before stabilizing. The co-infected population grows gradually as both diseases spread and later stabilizes at a small persistent level due to recovery and removal. The recovered population steadily increases as individuals recover from infection and eventually stabilizes when recovery balances natural death. Environmental bacteria initially increase due to shedding from infected individuals but later decline and stabilize because of the bacteria clearance rate.

In figure 2, the model confirms the epidemic threshold property: infections die out when reproduction numbers are less than one and persist at endemic levels when they exceed one. Figure 3 shows two scenarios were illustrated: when reproduction numbers are below unity, infections decline to zero; when they exceed unity, infections persist and stabilize at endemic levels. Figure 4 illustrated an increase in the Typhoid transmission rate significantly increases infection levels, showing that it strongly influences disease spread as seen in Alhassan et al. (2021). Figure 5 also show an increase in the HCV transmission rate that also raises infection levels, particularly co-infection, although its effect is slightly weaker than Typhoid transmission. Higher Typhoid recovery rates reduce infection prevalence, while lower



recovery rates allow infections to persist longer shown in Figure 6. Figure 7 demonstrated increase in the HCV recovery rate also reduces infection levels, though the effect is more gradual due to the slower progression of HCV. Higher environmental bacteria clearance reduces infection levels, highlighting the importance of sanitation in controlling Typhoid transmission as seen in Figure 8.

## CONCLUSION

This study developed and analyzed a mathematical model for the co-infection dynamics of Hepatitis C Virus (HCV) and Typhoid fever. The model incorporated human infection compartments and environmental bacteria to describe the interaction between the two diseases. The results show that Typhoid spreads more rapidly due to environmental transmission, while HCV progresses more slowly but maintains longer infectious periods. Co-infection occurs when both diseases coexist in the population and stabilizes at a lower endemic level. The analysis also confirms the threshold phenomenon: infections die out when reproduction numbers are below one and persist when they exceed unity. Sensitivity analysis further shows that transmission rates, recovery rates, and environmental sanitation significantly influence disease prevalence. Overall, reducing transmission, improving treatment and recovery, and strengthening environmental sanitation are key strategies for controlling Typhoid, HCV, and their co-infection.

## REFERENCES

- Abah, R. T. (2023). Mathematical modeling and simulation for controlling typhoid fever disease. *International Journal of Recent Research in Mathematics Computer Science and Information Technology*, 10(1), 46–56.
- Abdulai, K., & Baba, S. (2023). Mathematical model on the transmission dynamics of typhoid fever with treatment and booster vaccination. *Applied Mathematics and Statistics*, 1–14.
- Abegye, S. Y., & Kpanja, S. S. (2023). Sensitivity analysis of mathematical modeling of tuberculosis dynamics with a control measure. *African Journal of Mathematics and Statistics Studies*, 6(3), 17–34.
- Alhassan, et al. (2021). Mathematical model for the transmission dynamics of typhoid fever infection with treatment. *International Journal of Science for Global Sustainability*, 7(2), 37–49.
- Avendaño, J., et al. (2002). Mathematical model for the dynamics of hepatitis C. *Journal of Theoretical Medicine*, 4(2), 109–118.
- Daniel, et al. (2025). Mathematical modeling and analysis of COVID-19 and typhoid fever co-dynamics with treatment. *Scientific Reports*, 5(2), 1–20.
- Elamin, H. E. (2013). Model for hepatitis C virus transmission. *Mathematical Biosciences and Engineering*, 10(4), 1045–1065.
- Elaydi, S., & Lozi, R. (2024). Global dynamics of tuberculosis discrete mathematical models. *Journal of Biological Dynamics*, 18(4), 246–273.
- Enejoh, et al. (2026). Numerical solution of fractional order typhoid fever model via the generalized fractional Adams–Bashforth–Moulton approach. *Network Modeling Analysis in Health Informatics and Bioinformatics*, 5(2), 16–41.



- Inayaturohmat, et al. (2022). A mathematical modeling of tuberculosis and COVID-19 coinfection with the effect of isolation and treatment. *Applied Mathematics and Statistics*, 12(3), 1–13.
- Joshua, E., Akpan, E., & Inyang, U. (2024). Mathematically modeling and computational dynamics of the impact of quasi-lockdown policy in control of COVID-19 in Akwa Ibom State, Nigeria. *Asian Research Journal of Mathematics*, 20(1), 22–48.
- Konlan, M. (2024). Global stability analysis and modeling onchocerciasis transmission dynamics with control measures. *Infection Ecology & Epidemiology*, 14(1), 234–347.
- Lunga, M., & Farai, N. (2022). Mathematical analysis of cholera–typhoid co-infection transmission dynamics. *Applied Mathematics and Statistics*, 6(2), 1–13.
- Lunga, M. F. (2021). Mathematical analysis of typhoid fever transmission dynamics with seasonal and fear effects. *Communications in Mathematical Biology and Neuroscience*, 5(3), 1–28.
- Mamo, S. W., Purnachandra, R. K., & Alemu, G. W. (2022). Mathematical modeling of co-infections of hepatitis A viral disease and typhoid fever with optimal control strategies. *Nonlinear Analysis and Applications*, 13(2), 899–921.
- Mlyashimb, H., Josiah, M., & Adquate, M. (2025). A mathematical model of HCV transmission dynamics with sex stratification and environmental effects. *PLoS ONE*, 20(12), 1–21.
- Muhammad, et al. (2023, August 3). *Mathematical model of typhoid disease using standard and non-standard finite difference schemes*. <https://doi.org/10.21203/rs.3.rs-3205528/v1>
- Nisar, et al. (2024). Computational and stability analysis of Ebola virus epidemic model with piecewise hybrid fractional operator. *International Journal of Environmental Research and Public Health*, 19(4), 67–92.
- Nthiiri, J. K., et al. (2016). Mathematical modelling of typhoid fever disease incorporating protection against infection. *British Journal of Mathematics & Computer Science*, 14(1), 1–10.
- Olajide, et al. (2025). Sociodemographic characteristics and risk factors for hepatitis B and C virus infections: Salmonella serovars in participants' blood samples in Uyo, Nigeria. *Microbes and Infectious Diseases*, 7(2), 12–15.
- Oluwakemi, et al. (2022). Mathematical modeling of HIV–HCV co-infection model: Impact of parameters on reproduction number. *Journal of Applied Mathematics and Statistics*, 12(5), 23–39.
- Omowumi, F., Tunde, T., & Afeez, A. (2024). On mathematical modelling of optimal control of typhoid fever with efficiency analysis. *Journal of the Nigerian Society of Physical Sciences*, 6(2), 1–12.
- Singh, et al. (2023). Mathematical modelling and analysis of COVID-19 and tuberculosis transmission dynamics. *Informatics in Medicine Unlocked*, 6(2), 123–139.
- Sulayman, et al. (2019). Mathematical model and stability analysis of typhoid fever. *Lapai Journal of Applied and Natural Sciences*, 4(1), 47–54.
- Sunday, et al. (2023). Mathematical modelling of spread and control of the hepatitis C virus. *International Journal of Science and Research (IJSR)*, 12(5), 581–588.
- Thierry, et al. (2025). Mathematical modelling of the dynamics of typhoid fever and two modes of treatment in a health district in Cameroon. *Mathematical Biosciences and Engineering*, 22(2), 477–510.
- World Health Organization. (2024). *Typhoid: Fact sheet*. <https://www.who.int/news-room>
- World Health Organization. (2025). *Transfusion transmitted infections*. <https://www.who.int/news-room>
- Zelege, A. J., & Temesgen, T. (2021). Mathematical modeling of co-infection of typhoid fever and *Plasmodium falciparum*. *IOSR Journal of Mathematics (IOSR-JM)*, 17, 35–56.